

Evidence of Lévy stable process in tokamak edge turbulence

R. Jha¹, P. K. Kaw¹, D. R. Kulkarni², J. C. Parikh², and ADITYA Team¹

1. Institute for Plasma Research, Bhat, Gandhinagar-382 428, INDIA
2. Physical Research Laboratory, Navarangpura, Ahmedabad- 380 009, INDIA

ABSTRACT

In an effort to understand the fundamental physics of turbulent transport of particles and heat in a tokamak, the floating potential fluctuations in the the scrape-off layer plasma of ohmically heated ADITYA tokamak are analysed for self-similarity using distribution function approach. It is observed that the distribution function of a sum of n data points converges to a Lévy distribution of scale index, $\alpha = 1.111$ for $n \leq 40$ and $\alpha = 2.0$ for larger n . In both scaling ranges, the edge fluctuation is self-similar. This observation is backed by several supporting evidences. The results indicate that the small scale fluctuations transport matter and heat dominantly by convection whereas the transport due to large scale fluctuations is by a diffusive process.

PACS numbers: 52.35.Ra, 47.27.Qb, 05.40.Fb

Experimental observations [1] and numerical simulations [2] have shown that random fluctuations in the edge plasma of a tokamak exhibit a tendency to organize themselves into coherent structures. These structures are expected to play an important role in causing transport of particles, a topic of considerable interest in modern fusion devices. The measurement of fluctuation induced particle flux shows bursty nature [3]. An attempt has been made to explain the bursty nature of particle transport in terms of self organized criticality (SOC) as indicated by the observation of long range time correlation and self similarity in the fluctuation data [4]. However, whether or not the long range correlation is a manifestation of SOC (and a breakdown of the standard transport paradigm) is an open question [5].

In this paper, we carry out an additional investigation of bursty nature of particle transport in tokamak in terms of Lévy flights. The paradigm of Lévy flight has been used recently to explain anomalous transport in such diverse subjects as fluid dynamics [6], transient polymers [7], subrecoil laser cooling [8], human heart beat [9], movement of stocks in financial markets [10,11] and fluid turbulence [12]. The Lévy scale index, α is intimately related to the index, ν of the transport equation : $\langle R^2(t) \rangle = Dt^\nu$, where $\langle R^2(t) \rangle$ is the mean square distance travelled by the test particle in the random field in time t and D is the transport coefficient. For a diffusive transport, $\nu = 1$ whereas $\nu > 1$ indicates anomalous transport. In general, $\alpha = 2/\nu$ and hence $0 \leq \alpha < 2$ represents anomalous transport [13]. To demonstrate Lévy process and the resultant self- similarity, we have followed the approach of probability distribution function (PDF) [10,11]. This approach is superior because the PDF involves the entire range of fluctuation amplitude unlike the rescaled range (R/S) analysis which essentially describes the two point function of the PDF [4]. We provide evidence of a self- similar non-Gaussian process, which is a Lévy process, over a range of time scales up to 3 times the correlation time (τ_{ac}). At longer time scales the process is Gaussian. The observation implies a new paradigm of turbulent transport in tokamaks, viz., anomalous transport at short time scales and diffusive transport at larger time scales.

It has been shown by Lévy [14] that the sum of n independent stochastic variables, with a probability distribution having power-law wings, converges to a stable process characterized by the Lévy distribution. The process is stable because the PDF of the sum, $Z_n = \sum_{i=1}^n X_i$, of the stochastic variables $\{X\}$, has the same functional form as the PDF of X_j . The PDF

of a symmetrical Lévy stable process is given by [15,16]

$$p(Z_n) = \frac{1}{\pi} \int_0^\infty \exp(-n\gamma q^\alpha) \cos(qZ_n) dq \quad (1)$$

where α ($0 < \alpha \leq 2$) and γ (> 0) are the scale index and scale factor respectively. If the central region of the distribution is well described by a Lévy stable process, then the the probability of return to the origin is given by [10]:

$$p(Z_n = 0) = \frac{\Gamma(1/\alpha)}{\pi\alpha(n\gamma)^{1/\alpha}} \quad (2)$$

where Γ is a Gamma function. The Lévy stable symmetrical distributions rescale under the following transformations:

$$Z_s = \frac{Z_n}{n^{1/\alpha}} \quad (3)$$

and

$$p_s(Z_s) = n^{1/\alpha} p(Z_n) \quad (4)$$

Although Lévy stable process is characterized by infinite variance, the existence of finite variance in physical systems is treated either by introduction of spatiotemporal coupling [13] or by means of truncated Lévy distribution (TLD) where an exponential tail is imposed on the values of the stochastic variable [15,16]. The TLD is a Lévy stable process. In this paper, we report the evidence of a Lévy stable process in the turbulent edge plasma of ohmically heated ADITYA tokamak.

For this experiment, ADITYA tokamak is operated with with the following discharge parameters: plasma current, $I_p = 64 \pm 4$ kA, toroidal magnetic field at axis, $B_T = 0.75$ T, chord averaged plasma density, $\bar{n}_e = 1 \times 10^{19} m^{-3}$, major radius, $R_0 = 0.75$ m, minor radius, $a = 0.25$ m. The floating potential is measured using a poloidal array of Langmuir probes made up of molybdenum wires (length = 3.5 mm, diameter = 1 mm, separation = 3 mm) and located in the Scrape-off layer plasma 3 mm behind the limiter. The probes on a movable shaft are mounted on the top port, toroidally 72° away from the limiter in the electron side. The data are aquired at a sampling rate of 1 MHz in the time window 25-49 ms. The mean potential lies between -4 to 1 volts. The fluctuation data are generated after removing the 1 ms running average. With this procedure, we expect to remove the very low frequency fluctuations which are not part of plasma turbulence. A stationary

segment of data during 35-49 ms are chosen from seven discharges (8746-48 and 8752-55) for further analysis. The autocorrelation time, $\tau_{ac} = 12 \mu\text{s}$. The autocorrelation function falls sharply and crosses zero at about $t/\tau_{ac} = 2$ with no evidence of algebraic tail.

For further analysis, stationary fluctuation time series from 7 discharges are normalized with their root mean square (RMS) amplitude and stacked together. The distribution function is obtained using 980000 data points. This is shown in Fig.(1), together with a Gaussian having the same variables. The PDF of the fluctuation is nearly symmetrical (skewness = -0.38) but has a non-negligible kurtosis (1.24). The evidence of high kurtosis is seen in the distribution peaked near the origin. We next try to fit the PDF of the fluctuations data to a Lévy distribution.

In order to determine the Lévy scale index α , the number of convolutions is chosen in the logarithmic intervals, $n = 2^{i-1}$, where $i = 1, 2, \dots, 11$. The original time series is divided into non-overlapping blocks of n data points and a new variable, Z_n is generated for each block. The new time series is then subjected to Lévy analysis. The probability of return to origin, $p(Z_n = 0)$ is plotted as a function of n . This is done for the following reasons: (i) the distribution function is most accurate at $Z_n = 0$, and (ii) the analytical form of only $p(Z_n = 0)$ is known [Eq.(2)]. It is observed that on a log-log plot (Fig. 2), there are two clear slopes with values -0.9 and -0.5 in the n -ranges 1-40 and 40-500 respectively. The slope with value -0.9 corresponds to Lévy index $\alpha = 1.111$ and that with value -0.5 to $\alpha = 2.0$. The values of the scale factor, γ in the two scaling ranges are 0.64 ± 0.06 and 8.03 ± 0.76 respectively. It is important to note that the cross-over to a Gaussian process takes place at $n = n_x = 40$ which is much larger than that expected from the central limit theorem [17].

In Fig.(3a) we compare the PDF observed for $n=1$ with the Lévy stable distribution of the scale index, $\alpha=1.111$ and scale factor, $\gamma=0.59$. The Lévy distribution is a good fit in the central region of the PDF upto 3σ values of the stochastic variable. Beyond 3σ , the PDF departs from both Lévy and Gaussian forms. Note that the values of α and γ are obtained in the self-similarity range of $n=1-32 \mu\text{s}$. This range represents small scale fluctuations in the floating potential. Figure 3(b) shows the full distribution function for the n -values 1, 2, 4, 8, 16 and 32. As the number of convolutions increases, the distribution function becomes broad and the peak

value (or, the probability of return to origin) decreases. If the stochastic variable, Z_n and the distribution function, $p(Z_n)$ are rescaled in accordance with Eq.(3) and Eq.(4) respectively, the distribution functions, $p_s(Z_s)$ collapse on $n = 1$ distribution (Fig. 3(c)). Thus, the distribution functions of different convolutions are self-similar in the range $n = 1$ to 32. A self-similarity is also obtained for n -values 64, 128, 256 and 512 by using $\alpha=2.0$ and $\gamma=8.03\pm 0.76$. Figure 4 shows the rescaled distribution functions in the two scaling regimes on the same graph. The difference of $\log(p_s(Z_s = 0))$ values in the first and the second scaling regimes provides a measure of the 'distance', Δ between the two scaling regimes [15]. The $\Delta \approx 0.6$ for the results shown in Fig. 4 indicates that the 'distance' is significantly large.

We have verified the above results by carrying out the following analysis: (i) the root mean square (RMS) amplitude of the stochastic variable (Z_n), σ_{Z_n} shows a power-law behaviour, $\sigma_{Z_n} \sim n^{\nu/2}$. The exponent, $\nu=1.8$ in the short time scaling range ($n=1-32$) whereas, $\nu=1.0$ in the long time scaling range ($n=100-800$). Thus, the small scale fluctuations show non-Gaussian PDF and a self-similar scaling behaviour. The long scales show self-similarity of Gaussian type. It can be argued that the RMS amplitude of potential fluctuation is proportional to the root mean square distance travelled by a test particle in the random field [18]. (ii) the rescaled range (R/S) analysis on the combined data set shows a somewhat longer scaling range at short time scales ($n= 1-128$) having Hurst parameter, $H=0.9$. At long time scales, $n=256-4096$, the value of $H = 0.6$. One is tempted to interpret it as an evidence of long range self-similarity of non-Gaussian type. However, it should be pointed out that R/S range analysis has tendency to give somewhat higher values of H [19]. Therefore, we consider that at long time range, the fluctuation data show self-similarity of Gaussian type. (iii) when we calculate the kurtosis (K) of the time series corresponding to different convolutions (n), it is observed that kurtosis decreases with increasing n and $K < 0.2$ for $n > 60$. This result is similar to those reported earlier in tokamak [20] and stellerator [21]. Thus, the small scale fluctuations are non-Gaussian whereas the large scales are Gaussian.

In conclusion, we have presented evidences of a Lévy stable process in tokamak edge turbulence. The sum of n data points of a fluctuation time series converges to a Lévy distribution of scale index, $\alpha=1.111$ for $n \leq 40$ and $\alpha= 2.0$ for larger n . The probability distribution functions are self similar in both scaling ranges. This observation is backed by several supporting

evidences.

We finally give a possible interpretation of these observations and speculate on their implication for the problem of bursty transport due to turbulence in the tokamak edge region. We have earlier carried out conditional statistical analysis of Langmuir probe data in the edge of tokamak ADITYA (for similar discharges) and shown that the fluctuations are dominated by coherent structures which appear intermittently in space and time, typically lasting 25-30 μs and having poloidal scale lengths of a few cm. These structures are also associated with sharp radial potential gradients separating the last closed magnetic surface from the scrape-off layer plasma. Bursts of turbulent transport into the scrape-off layers are related to intermittent breakdown of radial confinement and the coherent structures extending into the open field line regions. We believe that the non-gaussian PDFs of potential fluctuation (ϕ) described above are due to such coherent structures. For time scales longer than the life time ($\approx 25\text{-}30 \mu\text{s}$), we observe only a randomized average behaviour and hence infer only Gaussian statistics and diffusive behaviour. For shorter time scales, on the other hand, convective effects due to coherent structures dominate and we observe the anomalous behaviour, $\langle R^2 \rangle \sim t^\nu$ with $\nu=1.8$. We may also make an estimate of the enhancement of turbulent transport due to convective effects introduced by the presence of coherent eddy-like structures by using the analysis of Rosenbluth et al. [22]. The enhancement factor $f = D^*/D \sim P^{1/2}$ where the Peclet number $P \sim vd/D$ is the ratio of the diffusion time to the eddy turnover time. For a typical eddy size of $d \sim 1$ cm, the typical eddy velocity, $v \sim cE/B \sim 10^5$ cm/s and diffusion coefficient, $D \sim 10^4$ cm²/s [1,23], we find an enhancement factor $f \sim 3$. Thus, the presence of transient coherent eddies can give sudden avalanche-like enhancements of transport by a factor of 3 or more, resulting in bursty nature of transport.

REFERENCES

- (1) B. K. Joseph et al., Phys. Plasmas **4**, 4292 (1997); S. Benkadda et al., Phys. Rev. Lett. **73**, 3403 (1994).
- (2) A. E. Koniges et al., Phys. Fluids B **4**, 2785 (1992); J. A. Crotinger and T. H. Dupree, Phys. Fluids B **4**, 2854 (1992).
- (3) M. Endler et al. Nucl. Fusion **35**, 1307 (1995).
- (4) B. A. Carreras et al., Phys. Rev. Lett. **80**, 4438 (1998); B. A. Carreras et al., Phys. Plasmas **5**, 3632 (1998).
- (5) J. A. Krommes and M. Ottaviani, Phys. Plasmas **6**, 3731 (1999).
- (6) T. H. Solomon et al., Phys. Rev. Lett. **71**, 3975 (1993).
- (7) A. Ott et al., Phys. Rev. Lett. **65**, 2201 (1990).
- (8) F. Bardou et al., Phys. Rev. Lett. **72**, 203 (1994).
- (9) C. K. Peng et al., Phys. Rev. Lett. **70**, 1343 (1993).
- (10) R. N. Mantegna and H. E. Stanley, An Introduction to Econophysics, Cambridge University Press, U.K. (2000), p. 26.
- (11) R. N. Mantegna and H. E. Stanley, Nature **376**, 46 (1995); S. Ghashghaie et al., Nature **381**, 767 (1996);
- (12) M. F. Shlesinger et al., Phys. Rev. Lett. **58**, 1100 (1987).
- (13) A. Blumen, G. Zumofen and J. Klafter, Phys. Rev. A **40**, 3964 (1989).
- (14) P. Lévy, Théorie de l'Addition des Variables Aléatoires (Gauthier-Villars, Paris, 1937).
- (15) R. N. Mantegna and H. E. Stanley, Phys. Rev. Lett. **73**, 2946 (1994); R. N. Mantegna, Phys. Rev. E **49**, 4677 (1994).
- (16) J.-P. Bouchaud and M. Potters, Theory of financial risk: from data analysis to risk management, Cambridge University Press, U. K. (2000).
- (17) For a time series, $X_i = \cos(\theta_i)$, where θ_i is a uniformly distributed random phase in the range $0 - 2\pi$, the sum, $Z_n = \sum_1^n X_i$ becomes Gaussian for $n \geq 8$.

- (18) The tokamak edge plasma is dominated by low frequency electrostatic turbulence in which the radial displacement (R) is given by $\mathbf{E} \times \mathbf{B}$ motion, viz., $dR/dt = (1/RB)\partial\phi/\partial\theta$, where B is the magnetic field, ϕ is the electric potential. Noting further that the plasma has mean poloidal velocity of order v_0 , we find $R \approx \phi/v_0B$ indicating the potential ϕ is a direct measure of radial displacement.
- (19) B. A. Carreras et al., Phys. Plasmas **6**, 1885 (1999).
- (20) R. Jha et al., Phys. Rev. Lett. **69**, 1375 (1992); R. Jha and Y. C. Saxena, Phys. Plasmas **3**, 2979 (1996).
- (21) V. Carbone et al., Phys. Plasmas **7**, 445 (2000).
- (22) M. N. Rosenbluth et al., Phys. Fluids **30**, 2636 (1987).
- (23) R. Jha et al., Nucl. Fusion **33**, 1201 (1993).

FIGURE CAPTION

- (1) The probability distribution function (PDF) of floating potential fluctuation. The amplitude (Z) is normalized to the standard deviation. The symbol (open circle) shows the experimental data points whereas the dotted line shows a Gaussian PDF of unity standard deviation.
- (2) The probability of return to the origin, $p(Z_n = 0)$ as a function of the number of data points (n) in the non-overlapping blocks. For $n=1024$ and beyond, the PDF is not well defined and $p(Z_n = 0)$ estimates may be in error. Since we have filtered out time scales larger than 1 ms, they do not contribute to the PDF.
- (3) (a) The PDF, $p(Z)$ for the experimental data (bullets) together with the Gaussian distribution (dotted line) and the Lévy distribution (solid line), (b) the PDF, $p(Z_n)$ vs. Z_n for different n . The width of $p(Z_n)$ increases with increasing n , (c) the rescaled PDF, $p_s(Z_s)$ for the first six convolutions ($n = 1-32$).
- (4) The comparison of rescaled PDF, $p_s(Z_s)$ in the scaling ranges, $n = 1-32$ (solid lines, without symbol) and $n = 64-512$ (with symbols).

Figure 1

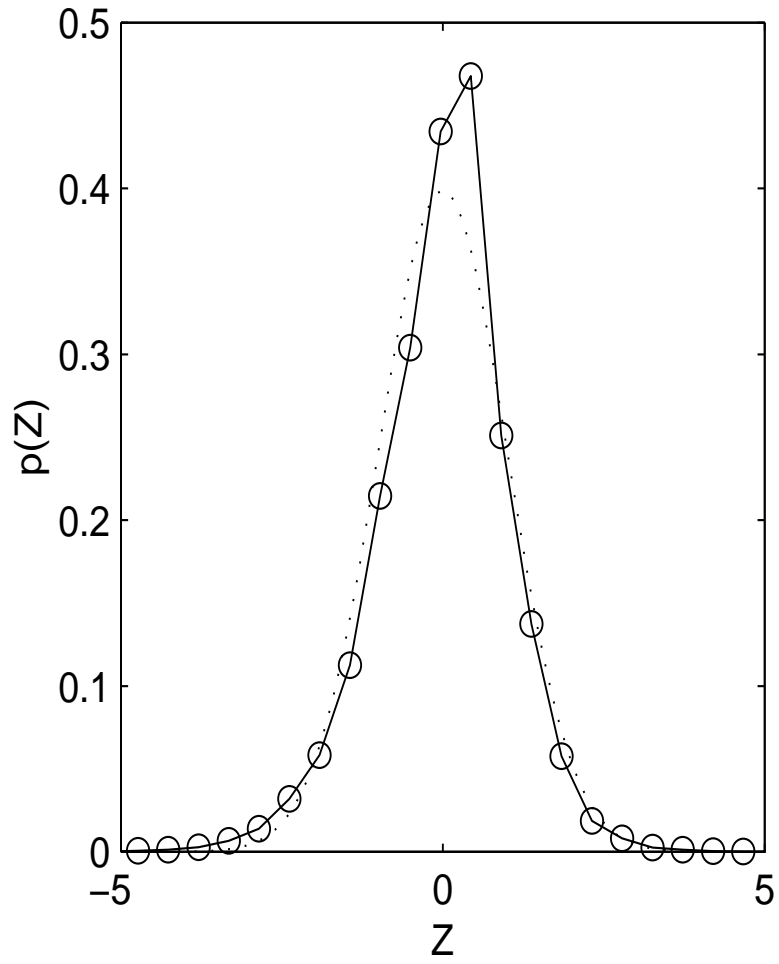


Figure 2

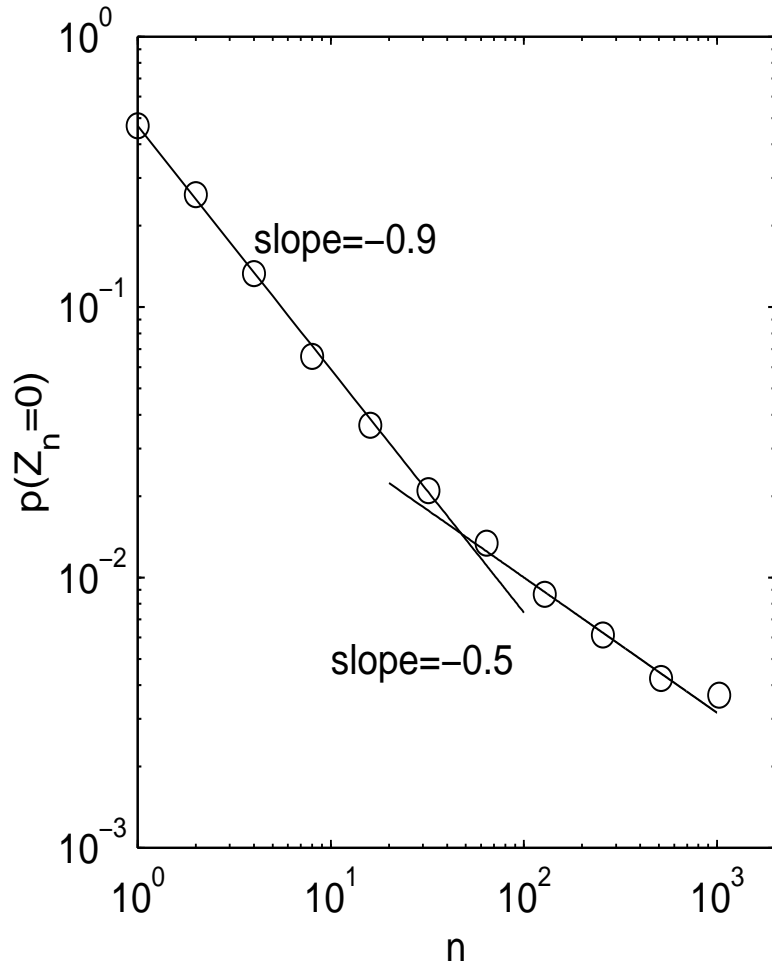


Figure 3

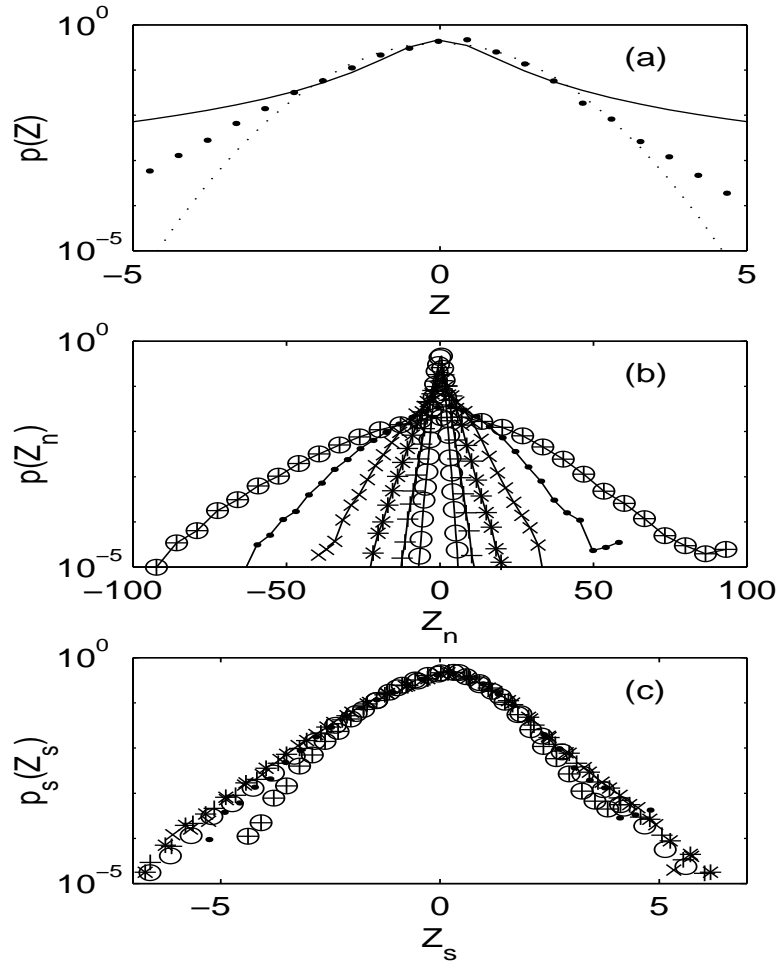


Figure 4

